LOGIT MARGIN MATTERS: IMPROVING TRANSFERABLE TARGETED ADVERSARIAL ATTACK BY LOGIT CALIBRATION

Anonymous authors
Paper under double-blind review

ABSTRACT

Previous works have extensively studied the transferability of adversarial samples in untargeted black-box scenarios. However, it still remains challenging to craft the targeted adversarial examples with higher transferability than non-targeted ones. Recent studies reveal that the traditional Cross-Entropy (CE) loss function is insufficient to learn transferable targeted perturbations due to the issue of vanishing gradient. In this work, we provide a comprehensive investigation of the CE loss function and find that the logit margin between the targeted and untargeted classes will quickly obtain saturation in CE, which largely limits the transferability. Therefore, in this paper, we devote to the goal of enlarging logit margin and propose two simple and effective logit calibration methods, which are achieved by downscaling the logits with a temperature factor and an adaptive margin, respectively. Both of them can effectively encourage the optimization to produce larger logit margin and lead to higher transferability. Besides, we show that minimizing the cosine distance between the adversarial examples and the classifier weights of the target class can further improve the transferability, which is benefited from downscaling logits via L2-normalization. Experiments conducted on the ImageNet dataset validate the effectiveness of the proposed methods, which outperform the state-of-the-art methods in black-box targeted attacks. The source code is available at Link.

1 INTRODUCTION

In the past decade, deep neural networks (DNNs) have achieved remarkable success in various fields, *e.g.*, image classification (Simonyan and Zisserman, 2015), image segmentation (Long et al., 2015), and object detection (Ren et al., 2015). However, Goodfellow et al. (2015) revealed that the DNNs are vulnerable to adversarial attacks, in which adding imperceptible disturbances to the input can lead the DNNs to make an incorrect prediction. Many following approaches (Dong et al., 2018; 2019; Cohen et al., 2019; Tramèr et al., 2018; Xie et al., 2019) have been proposed to construct more destructive adversarial samples for investigating the vulnerability of the DNNs. Goodfellow et al. (2015); Liu et al. (2016) also showed that the adversarial samples are transferable across different networks, raising a more critical robustness threat under the black-box scenarios. Therefore, it is vital to explore the vulnerability of the DNNs, which is very useful for designing robust DNNs.

Currently, most of the works (Dong et al., 2018; Xie et al., 2019; Lin et al., 2020; Huang et al., 2019; Wu et al., 2020; Guo et al., 2020) have been devoted to the untargeted black-box attacks, in which adversarial examples are crafted to fool unknown CNN models predicting unspecified incorrect labels. For example, Dong et al. (2018); Xie et al. (2019) leveraged input-level transformation or augmentation to improve the non-targeted transferability. Huang et al. (2019) proposed a powerful intermediate feature-level attack. Wu et al. (2020); Guo et al. (2020) demonstrated that backpropagating more gradients through the skip-connections can increase the transferability. Despite the success in non-targeted cases, the targeted transferability remains challenging, which requires eliciting the black-box models into a pre-defined target category.

For learning the transferable adversarial samples in untargeted cases, most methods have leveraged the Cross-Entropy (CE) as the loss function. However, Li et al. (2020); Zhao et al. (2021) recently showed that the CE loss is insufficient for learning the adversarial perturbation in the targeted case due to the issue of vanishing gradient. To deal with this issue, Li et al. (2020) adopted the Poincaré

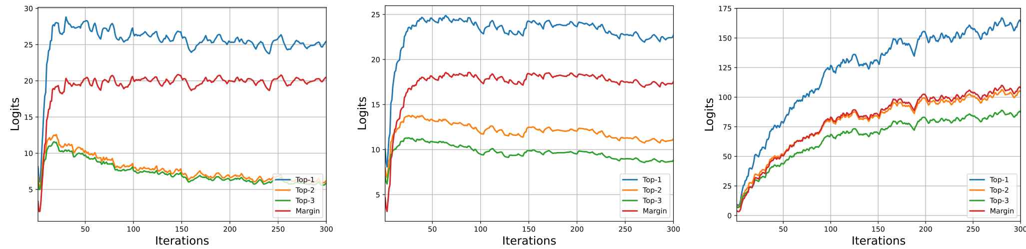

(a) Cross-Entropy (b) Po+Trip (c) Logit

Figure 1: The average Top-3 logits and logit margin of 50 adversarial samples trained by the Cross-Entropy, Po+Trip (Li et al., 2020) and Logit (Zhao et al., 2021) loss functions for crafting the ResNet-50. (* Training and computation details of this figure are in Section 3.1)

distance to increase the gradient magnitude during the optimization adaptively. Zhao et al. (2021) demonstrated that an effortless logit loss equal to the negative value of the targeted logits could alleviate the gradient issue and achieve surprisingly strong targeted transferability. Besides, Zhao et al. (2021) also showed that optimizing with more iterations can significantly increase the targeted transferability. Although Zhao et al. (2021) demonstrated that continually enlarging the logit of the targeted class (as shown in Fig. 1(c)) can improve the transferability of adversarial samples, it still does not thoroughly analyze the insufficient issue in the CE loss function.

In this study, we take a closer look at the vanishing gradient issue in the CE loss function and find that the logit margin between the targeted and non-targeted classes will quickly get saturated during the optimization (as shown in Fig. 1(a)). Moreover, this issue will influence the attack performance of the perturbations and thus essentially limits the transferability. Specifically, along with the training iterations in CE, we observe that the logits of the targeted and non-targeted classes increase rapidly in the first few iterations. However, after reaching the peak, the logit margin between the targeted and non-targeted classes will get saturated, and further training will decrease the logits simultaneously to maintain this margin. This phenomenon is mainly due to the fact that the softmax function in CE will approximately output the probability of the target class to 1 when reaching the saturated margin (*e.g.*, 10). Thus, it raises the problem that the transferability will not be further increased even with more optimization iterations. A similar saturated phenomenon can be observed in the Po+Trip loss as shown in Fig. 1(b) (Li et al., 2020). While in practice, we are encouraged to increase the transferability by maximizing both the logits for the targeted class and its margin against other non-targeted classes to cross the decision boundaries of other black-box models.

In this paper, we devote to enlarging logit margins to alleviate the above saturation issue in CE. Inspired by the temperature-scaling used in the knowledge distillation (Hinton et al., 2015), a higher temperature T will produce a softer probability distribution over different classes. We firstly leverage this scaling technique into the targeted attack to calibrate the logits. Then the logits margin between the targeted and non-targeted classes will not be saturated after only a few iterations and will keep improving the transferability. On the other aspect, instead of using a constant T, we further explore an adaptive margin-based calibration by scaling the logits based on the logit margin of the target class and the highest non-target class. In addition, we also investigate the effectiveness of calibrating the targeted logit into the unit length feature space by L2-normalization, which is equivalent to minimizing the angle between the adversarial examples and the classifier of targeted class.

Finally, we conduct experiments on the ImageNet dataset to validate the effectiveness of the logits calibration for crafting transferable targeted adversarial examples. Experimental results demonstrate that the calibration of the logits helps achieve a higher attack success rate than other state-of-the-art methods. Besides, the combination of different calibrations can further provide mutual benefits.

2 Related Works

In this section, we give a brief introduction of the related works from the following two aspects: *untargeted black-box attacks* and *targeted attacks*.

2.1 UNTARGETD BLACK-BOX ATTACKS

After Szegedy et al. (2015) exposed the vulnerability of deep neural networks, many attack methods (Xie et al., 2019; Dong et al., 2019) have been proposed to craft highly transferable adversaries in the non-targeted scenario. We first review several gradient-based attack methods that focus on enhancing the transferability against black-box models.

Iterative-Fast Gradient Sign Method (I-FGSM) (Kurakin et al., 2018) is an iterative version of FGSM Goodfellow et al. (2015), which adds a small perturbation with a small step size α in the gradient direction iteratively:

$$\hat{x}_0 = x, \quad \hat{x}_{i+1} = \hat{x}'_i + \alpha \cdot \mathrm{sign}(\nabla_{\hat{x}} J(\hat{x}'_i, y)), \tag{1}$$

where $\hat{x}'_i$ denotes the adversarial image in the i_{th} iteration, $\alpha = \epsilon/T$ ensures the adversaries are constrained within an upper-bound perturbation ϵ through the l_p-norm when optimized by T iterations.

Following the seminal I-FGSM (Kurakin et al., 2018), a series of methods have been proposed to improve the transferability of attacking black-box models from different aspects, *e.g.*, gradient-based, input augmentation-based. For example, the **Momentum Iterative-FGSM (MI-FGSM)** (Dong et al., 2018) introduces a momentum term to compute the gradient of the I-FGSM, encouraging the perturbation is updated in a stable direction. The **Translation Invariant-FGSM (TI-FGSM)** (Dong et al., 2019) adopts a predefined kernel W to convolve the gradient $\nabla_{\hat{x}} J(\hat{x}'_i, y)$ at each iteration t, which can approximate the average gradient over multiple randomly translated images of the input $\hat{x}_t$. On the other aspects, the **Diverse Input-FGSM (DI-FGSM)** (Xie et al., 2019) leverages the random resizing and padding to augment the input $\hat{x}_t$ at each iteration. Currently, most targeted attack methods Li et al. (2020); Zhao et al. (2021); Naseer et al. (2021) simultaneously use the MI, TI and DI to form a strong baseline with better transferability.

2.2 TARGETED ATTACKS

Targeted attacks are different from non-targeted attacks, which need to change the decision to a specific target class. Kurakin et al. (2016) integrates the above non-targeted attack methods into targeted attacks to craft targeted adversarial examples. However, the performance is limited because it is insufficient to fool the black-box model only by maximizing the probability of the target class with the CE loss.

Po+Trip (Li et al., 2020) finds the insufficiency of CE is mainly due to vanishing gradient issue. Then, Li et al. (2020) leverages the Poincaré space as the metric space and further utilizes Triplet loss to improve targeted transferability by forcing adversarial example toward the target label and away from the ground-truth label. To further address this gradient issue, **Logits** (Zhao et al., 2021) adopts a simple and straightforward idea by directly maximizing the target logit to pull the adversarial examples close to the target class, which can be expressed as:

$$L_{Logit} = -z_t(\boldsymbol{x}'), \tag{2}$$

where $z_t(\cdot)$ is the output logits of the target class.

On the other hand, many studies employ resource-intensive approaches to achieve targeted attacks, which train target class-specific models (auxiliary classifiers or generative models) on additional large-scale data. For example, the FDA methods (Inkawhich et al., 2020b;a) use the intermediate feature distributions of CNNs to boost the targeted transferability by training class-specific auxiliary classifiers to model layer-wise feature distributions. The GAP (Poursaeed et al., 2018) trains a generative model for crafting targeted adversarial examples. Subsequently, Naseer et al. (2019) adopts a relativistic training objective to train the generative model for improving attack performance and cross-domain transferability. Recently, the TTP (Naseer et al., 2021) utilizes the global and local distribution matching for training target class-specific generators for obtaining high targeted transferability. However, the TTP requires actual data samples from the target class and brings expensive training costs. Different from the above methods, we introduce three simple and effective logit calibration methods into the CE loss function, which can achieve competitive performance without additional data and training.

3 METHOD

Problem Definition Given a white-box surrogate model $\mathbb{F}_s$ and an input x not from the targeted class t, our primary goal is to learn an imperceptible perturbation δ that can fool the $\mathbb{F}_s$ into output the target t for $\hat{x} = x + \delta$. Besides, the prediction of $\hat{x}$ will also be t when feeding to other unknown black-box testing models. The l_∞-norm is usually used to constrain the perturbation δ within an upper-bound ϵ, denoted as $||\delta||_\infty \leq \epsilon$.

For the surrogate model $\mathbb{F}_s$, we denote the feature for the final classification layer of the input x as $\phi(x)$. The logit z_i of the category i is computed by $z_i = W_i^T \phi(x) + b_i$, where W_i and b_i are the classifier weights and bias for category i. The corresponding probability p_i after the softmax function is calculated by $p_i = \frac{e^{z_i}}{\sum e^{z_j}}$.

3.1 LOGIT MARGIN

When successfully attacking the $\mathbb{F}_s$, the logit z_t of the target class t will be higher than the logits z_{nt} of any other non-target class in the classification task. Their logit margins can be computed by,

$$G(\phi(\hat{x})) = z_t - z_{nt} = W_t^T \phi(\hat{x}) + b_t - W_{nt}^T \phi(\hat{x}) + b_{nt}. \tag{3}$$

Li et al. (2020); Zhao et al. (2021) showed that it is insufficient to obtain transferable targeted adversarial samples that are only close to the target class while not far away enough from the true class and other non-targeted classes. Based on this property, it encourages us to continually enlarge this logit margin to increase the separation between the targeted and other non-targeted classes, thereby improving transferability.

To have a better understanding of the relationship between the logit margins and the targeted transferability, we visualize the average Top-3 logits (1 targeted class and other two non-targeted classes) of 50 random adversarial samples trained on ResNet50 by the CE, Po+Trip (Li et al., 2020), and the Logit (Zhao et al., 2021) loss functions with MI, DI and TI following. We also compute the average logit margin of the targeted class against the Top-20 non-targeted classes. The logit and the average logit margin are shown in Figure 1, and the transferability of these three loss functions from ResNet50 to VGG16 is plotted in Figure 2.

From Figure 1, we can observe that the logits of the targeted class and the Top-2 non-targeted classes increase rapidly in the first few iterations for the CE and Po+Trip loss, as well as their logit margins. When reaching the peak, the margin is saturated, and the logits start to decrease simultaneously to maintain the saturated margin. By comparing the CE and Po+Trip, the Po+Trip needs slightly more iterations to reach the saturated status and thus shows a marginal better transferability than CE, as shown in Figure 2. In comparison, the Logit loss function will keep increasing the logits of the targeted category and the logit margin. Thus, the Logit loss function shows a much better transfer targeted-attack success rate than CE and Po+Trip. On the other hand, the Logit loss also significantly increases the logits for other non-targeted classes when training with more iterations.

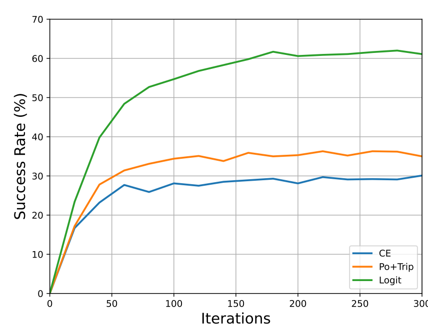

Figure 2: The targeted attack success rate (%) on VGG-16 by using the ResNet-50 as the surrogate model.

To further analyze why the logit margin will quickly reach saturated in the CE loss function and explore the effectiveness of increasing the margin during training, in the following sections, we will revisit the cross-entropy loss function and introduce the logit calibration to achieve this goal.

3.2 REVISITING THE CROSS-ENTROPY LOSS

Firstly, our objective is to maximize the logit margin in Eq. 3. After computing the gradient w.r.t. to $\phi(\hat{x})$, we can get

$$\frac{\partial G}{\partial \phi(\hat{x})} = W_t - W_{nt}. \tag{4}$$

This gradient indicates that the adversarial feature $\phi(\hat{x})$ needs to move towards the target class while apart from those non-target classes. Next, we compute the gradient w.r.t. to $\phi(\hat{x})$ in the Cross-Entropy loss function

$$L_{CE} = -\log(p_t) = -z_t + \log(\sum e^{z_j}), \tag{5}$$

and can get the gradient

$$\begin{aligned} \frac{\partial L_{ce}}{\partial \phi(\hat{x})} &= -\frac{\partial z_t}{\partial \phi(\hat{x})} + \frac{1}{\sum e^{z_j}} \cdot \frac{\partial \sum e^{z_j}}{\partial \phi(\hat{x})} \\ &= -\frac{\sum e^{z_i}}{\sum e^{z_j}} \cdot \frac{\partial z_t}{\partial \phi(\hat{x})} + \frac{1}{\sum e^{z_j}} \sum e^{z_i} \frac{\partial z_i}{\partial \phi(\hat{x})} \\ &= \sum \frac{e^{z_i}}{\sum e^{z_j}} \cdot (\frac{\partial z_i}{\partial \phi(\hat{x})} - \frac{\partial z_t}{\partial \phi(\hat{x})}) = \sum -p_i(W_t - W_i). \end{aligned} \tag{6}$$

From Eq. 6, we actually find that the CE loss is designed to adaptively optimize the $\phi(\hat{x})$ towards W_t and away from other W_i. However, after optimization with several iterations, the p_i of the non-targeted class will soon approach to 0 and then the influence of $W_t - W_i$ significantly vanishes.

Let's consider the case only with 2 classes (t and nt), we have the probabilities p_t and p_{nt} as:

$$p_t = \frac{e^{z_t}}{e^{z_t} + e^{z_{nt}}} = \frac{1}{1 + e^{-(z_t - z_{nt})}}, \tag{7}$$

$$p_{nt} = \frac{e^{z_{nt}}}{e^{z_t} + e^{z_{nt}}} = \frac{1}{1 + e^{(z_t - z_{nt})}}. \tag{8}$$

As shown in Figure 3, the p_t will get close to 1 when $z_t - z_{nt} > 6$ (*e.g.*, $p_{nt} \approx 2e^{-9}$ when $z_t - z_{nt} = 20$). In such a context, the gradient will significantly vanish. Recall that, in the CE loss function (Figure 1 (a)), the logit margin increases rapidly, but will reach saturated when approaching a certain value. This further indicates that the optimization of the CE loss function is largely restrained when the logit margin reaches a certain value.

To this end, we raise the question *if we explicitly enforce the optimization to enlarge the logit margin ($z_t - z_{nt}$), could we get better transferable targeted adversarial samples?*

To answer this, we propose to downscale the $z_t - z_{nt}$ by a factor s in the CE and extent the informative optimization for more iterations. Since in such circumstance, $z_t - z_{nt}$ will be enlarged by the factor s. Specifically, suppose that the optimization will be saturated when $z_t - z_{nt}$ reaches a certain value v. Using $z_t - z_{nt}$ and $\frac{z_t - z_{nt}}{s}$ in the CE will both approach the saturated value v. Then, it is easy to infer that, for the latter case, $z_t - z_{nt}$ will be $v \times s$.

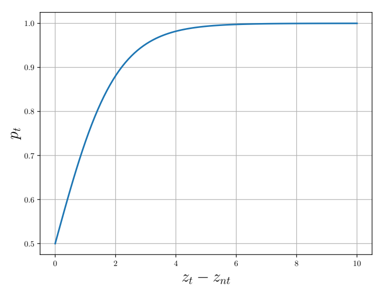

Figure 3: The probability of p_t under different $z_t - z_{nt}$.

3.3 Calibrating the Logits

To downscale the $z_t - z_{nt}$ during the optimization, we investigate three different types of logit calibrations in this study, *i.e.*, Temperature-based, Margin-based, and Angle-based.

3.3.1 Temperature-based

Inspired by the Temperature-scaling used in the knowledge distillation (Hinton et al., 2015), our first logit calibration directly downscales the logits by a constant temperature factor T,

$$\tilde{z}_i = \frac{z_i}{T}. \tag{9}$$

After introducing the T, the probability distribution $\boldsymbol{p}$ will be more softer over different classes. The corresponding gradient can be compute by:

$$\frac{\partial L_{ce}^T}{\partial \phi(\hat{x})} = \frac{e^{z_j/T}}{\sum e^{z_j/T}} \cdot \frac{1}{T}(\frac{\partial z_j}{\partial \phi(\hat{x})} - \frac{\partial z_t}{\partial \phi(\hat{x})}) = \sum -\hat{p}_i \frac{(W_t - W_i)}{T}. \tag{10}$$

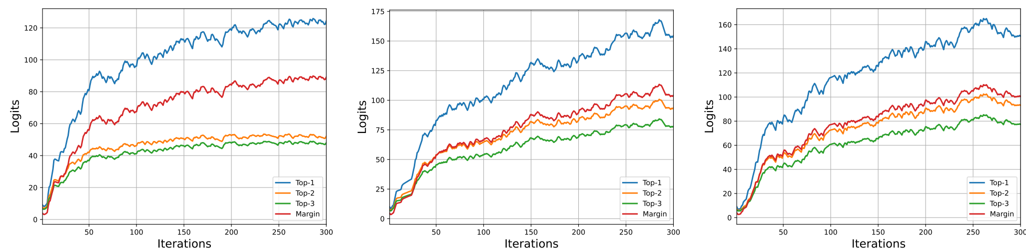

(a) T=5 (b) T=20 (c) Margin

Figure 4: The average Top-3 logits and logit margin of 50 adversarial samples after the logit calibration for crafting the ResNet-50.

After downscaling by the factor T, the new $\hat{p}_i$ after the softmax will not quickly approach to 0 when only trained with a few iterations.

In Figure 4 (a)(b), we visualize the trend of logits and margins of using $T = 5$ and $T = 20$. We can find that targeted logits and the logit margin will keep increasing as the same as the Logit in Figure 1. Meanwhile, the trend of $T = 20$ is very similar with the Logit (Zhao et al., 2021) and we show that the Logit loss function can be considered as a special case of calibrating the logits with a large T in the supplementary.

3.3.2 Margin-based

The previous Temperature-based logit calibration contains a hype-parameter T, which could be different for different surrogate model $\mathbb{F}_s$. To migrate this issue, we further introduce an adaptive margin-based logit calibration without extra hype-parameters. Specifically, we calibrate the logits by using the margin between the Top-2 logits in each iteration, denoted as:

$$\tilde{z}_i = \frac{z_i}{\hat{z}_1 - \hat{z}_2}, \tag{11}$$

where $\hat{z}_1$ and $\hat{z}_2$ are the Top-1 and the Top-2 logit, respectively.

In this Margin-based logit calibration, we will enforce the p_t and $p_{\hat{1}}$ of the Top-1 non-target class at each iteration meet the following constraints:

$$p_t = \frac{1}{1 + \sum_{i \neq t} e^{-(\tilde{z}_t - \tilde{z}_i)}} < \frac{1}{1 + e^{-1}}, \tag{12}$$

$$p_{\hat{1}} = \frac{1}{e^{\tilde{z}_{\hat{1}} - \tilde{z}_t} + \sum_{i \neq t} e^{\tilde{z}_i - \tilde{z}_{\hat{1}}}} > \frac{1}{N-1}(1 - \frac{1}{1 + e^{-1}}). \tag{13}$$

Then, it can adaptively deal with the vanishing gradient issue in the original CE loss function. The logits and the margin is shown in Figure 4 (c).

3.3.3 Angle-based

On the other aspect, the weights W_i for different category i usually has a different norm. To further alleviate the influence of various norms, we calibrate the logit into the feature space with unit length by L2-normalization, $\frac{W_i^T \phi(\hat{x}) + b_i}{||W_i||||\phi(x)||}$. If omit the b_i, this calibration is computed the $cos(\theta)$ between $\phi(\hat{x})$ and W_i, and we term it as angle-based calibration. *Since, this angle-based calibration will bound each logit smaller than one.* Instead of using the CE loss function, we directly minimize the angle between the $\phi(\hat{x})$ and the targeted weights W_t. The optimization loss function is:

$$L_{cosine} = -\frac{W_t^T \phi(\hat{x})}{||W_t||||\phi(\hat{x})||}. \tag{14}$$

The angle-based classifiers have been widely using in Face-Recognition task (Liu et al., 2017; Deng et al., 2019). In the experiments, we evaluate the performance of using different logit calibrations and their mutual benefits.

Table 1: The targeted transfer success rates (%) in the single-model transfer scenario. (Results with 20/100/300 iterations are reported, and the highest one at 300 iterations is showed **bold**.)

Attack	Surrogate Model: ResNet50			Surrogate Model: Dense121		
	→Dense121	→VGG16	→Inc-v3	→Res50	→VGG16	→Inc-v3
CE	27.0/40.2/42.7	17.4/27.6/29.1	2.3/4.1/4.6	12.3/17.2/18.4	8.6/10.5/10.9	1.6/2.3/2.8
Po+Trip	27.9/51.2/54.8	17.9/35.5/34.7	3.2/6.8/7.8	11.0/14.8/15.0	7.3/9.2/8.6	1.6/2.8/2.8
Logit	31.4/64.0/71.8	23.8/55.0/62.4	3.1/8.6/10.9	17.4/38.6/43.5	13.7/33.8/37.8	2.3/6.6/7.5
T=5	33.3/69.9/**77.8**	24.8/59.9/66.1	3.1/9.4/**12.2**	19.3/43.4/47.5	14.6/36.6/39.4	2.3/7.3/8.8
T= 10	31.6/68.5/77.0	23.6/58.5/**66.4**	2.8/9.4/11.6	17.9/43.2/**49.3**	13.4/36.8/**41.5**	2.2/7.7/8.8
Margin	33.3/65.8/76.5	23.1/58.6/65.7	3.0/9.5/12.2	18.8/42.8/47.2	14.5/36.5/41.4	2.5/7.7/**9.4**
Angle	38.9/72.5/77.2	29.2/60.7/65.2	4.4/10.7/11.1	20.6/43.2/47.8	16.5/35.7/39.3	3.0/7.7/8.9
Attack	**Surrogate Model: VGG16**			**Surrogate Model: Inc-v3**		
	→Res50	→Dense121	→Inc-v3	→Res50	→Dense121	→VGG16
CE	0.5/0.3/0.6	0.6/0.3/0.3	0/0/0.1	0.7/1.2/1.8	0.6/1.3/1.9	0.4/0.8/1.3
Po+Trip	0.7/0.6/0.7	0.7/0.6/0.5	0.1/0.1/0.1	1.0/1.6/1.7	0.6/1.7/2.5	0.7/1.2/1.8
Logit	3.4/9.9/11.6	3.5/12.0/13.9	0.3/1.0/**1.3**	0.6/1.1/2.0	0.6/1.9/3.0	0.6/1.5/2.8
T=5	3.1/7.0/6.9	3.3/7.6/7.8	0.2/0.9/0.8	0.7/1.7/2.1	0.5/1.9/**3.3**	0.4/1.6/2.6
T= 10	3.6/9.0/9.7	3.4/10.5/11.7	3.2/1.1/1.3	0.5/1.3/1.9	0.6/2.0/2.7	0.4/1.5/**2.8**
Margin	3.3/10.3/**12.0**	3.5/12.5/**14.5**	0.3/1.1/**1.3**	0.5/1.4/1.7	0.7/2.1/3.1	0.5/1.7/2.7
Angle	0.4/0.7/0.5	0.6/0.4/0.5	0/0/0.1	0.8/1.8/**2.6**	0.8/2.2/3.0	0.9/1.7/2.4

4 EXPERIMENTS

Experimental Setup. In this section, we evaluate the effectiveness of logit calibration for improving transferable targeted adversarial attack. Following the recent study (Zhao et al., 2021), we conduct the experiments on the difficult ImageNet-Compatible Dataset[1]. This dataset contains 1,000 images with 1,000 unique class labels corresponding to the ImageNet dataset. We implement our methods based on the source code[2] provided by the Logit (Zhao et al., 2021). The same four diverse CNN models are used for evaluation, *i.e.*, ResNet-50 (He et al., 2016), DenseNet-121 (Huang et al., 2017), VGG-16 with Batch Normalization (Simonyan and Zisserman, 2015) and Inception-v3 (Szegedy et al., 2016). The perturbation is bounded by $L_\infty \leq 16$. The TI (Dong et al., 2019), MI (Dong et al., 2018) and DI (Xie et al., 2019) are used for all attacks, and $||W||_1 = 5$ is set for TI. The I-FSGM is adopted for optimization with the $\alpha = 2$. The attacks are trained for 300 iterations on a NVIDIA-2080 Ti GPU. We run all the experiments for 5 times, and report the average targeted transfer success rates (%). Expect from the experiments in the following sections, more experimental results can be found in the supplementary of using the calibration in TTP (Naseer et al., 2021) and the non-targeted attack.

4.1 COMPARISON WITH OTHER METHODS IN SINGLE-MODEL TRANSFER

We first compare the proposed (temperature-based, margin-based and angle-based) logit calibrations with the original CE, Po+Trip (Li et al., 2020), and Logit (Zhao et al., 2021) in the single-model transfer task. In this task, we take one surrogate model for training, and test the targeted transferability in attacking other 3 models.

As shown in Table 1, the original CE loss function produces a worst performance than the Po+Trip and Logit. But after performing the logit calibration in the CE loss function, we can find a significant performance is boosted compared with the original CE. All the calibration methods can outperform the Logit, especially when using the ResNet50 and Dense121 as the surrogate model. These results indicate that the logit margin can significantly influence the performance of the targeted transferability. On the other aspect, we find that $T = 10$ has better performance than $T = 5$ on the VGG-16, suggesting that different models may need different T. Instead of finding the best T for a different model, the Margin-based calibration can solve the issue and reach the overall best transferability in all four models. However, we find that the Angle-based calibration is not working on the VGG16, which needs further investigation.

[1] https://github.com/cleverhans-lab/cleverhans/tree/master/cleverhans_v3.1.0/examples/nips17_adversarial_competition/dataset

[2] https://github.com/ZhengyuZhao/Targeted-Tansfer

4.2 The Influence of Different T in CE

In this section, we evaluate the influence of using different T in the CE loss function. The results are reported in Table 2. From the Table, we can have the following observations. **1)** The scaling factor T has a significant influence on the targeted transferability. Specifically, there is a large decrease in performance when using a small $T = 0.5$. After increasing the T, we can observe the number of successfully attacked samples will increase. **2)** The optimal T for different model is different. For example, $T = 5$ can produce the overall best performance for ResNet50, Dense121, and Inception v3, while the VGG16 with fewer convolutional layers requires a large T to obtain better transferability. **3)** The performances are comparable when using $T = 5$ and $T = 10$ for ResNet50, Dense121, and Inception v3. This is because that we use I-FSGM for optimization, which only considers the sign of the gradients. **4)** Using a larger T, the performance will be similar to the Logit loss function (see Table 1). We provide a deep analysis of this phenomenon in the supplementary material.

Table 2: The targeted transfer success rates (%) by using different T in CE loss function. (Results with 20/100/300 iterations are reported.)

Attack	Surrogate Model: ResNet50			Surrogate Model: Dense121		
	→Dense121	→VGG16	→Inc-v3	→Res50	→VGG16	→Inc-v3
T=0.5	13.2/16.0/19.5	7.1/9.5/11.0	1.2/1.8/2.4	4.2/5.0/6.2	2.5/3.5/3.2	0.6/0.9/1.1
T=1	27.0/40.2/42.7	17.4/27.6/29.1	2.3/4.1/4.6	12.3/17.2/18.4	8.6/10.5/10.9	1.6/2.3/2.8
T=2	34.2/62.8/67.7	24.4/52.3/53.9	3.3/7.2/8.5	18.7/35.0/36.1	13.2/27.3/27.0	2.2/5.5/6.1
T=5	33.3/69.9/**77.8**	24.8/59.9/66.1	3.1/9.4/**12.2**	19.3/43.4/47.5	14.6/36.6/39.4	2.3/7.3/8.8
T= 10	31.6/68.5/77.0	23.6/58.5/**66.4**	2.8/9.4/11.6	17.9/43.2/**49.3**	13.4/36.8/**41.5**	2.2/7.7/**8.8**
T = 20	30.4/65.6/74.3	22.9/55.4/63.6	3.2/9.0/11.6	17.6/40.3/46.2	13.4/35.4/40.1	2.3/6.7/8.7
Attack	Surrogate Model: VGG16			Surrogate Model: Inc-v3		
	→Res50	→Dense121	→Inc-v3	→Res50	→Dense121	→VGG16
T=0.5	0.2/0.1/0.2	0.1/0.1/0.1	0/0/0	0.3/0.9/0.9	0.3/0.8/1.4	0.3/0.6/1.3
T=1	0.5/0.3/0.6	0.6/0.3/0.3	0/0/0.1	0.7/1.2/1.8	0.6/1.3/1.9	0.4/0.8/1.3
T=2	1.6/1.8/1.8	1.8/1.9/1.6	0.2/0.2/0.2	0.6/1.5/2.0	0.4/1.7/2.2	0.5/1.2/2.0
T=5	3.1/7.0/6.9	3.3/7.6/7.8	0.2/0.9/0.8	0.7/1.7/2.1	0.5/1.9/3.3	0.4/1.6/2.6
T= 10	3.6/9.0/9.7	3.4/10.5/11.7	0.3/1.1/1.3	0.5/1.3/1.9	0.6/2.0/2.7	0.4/1.5/**2.8**
T = 20	3.4/9.7/**11.1**	3.6/12.7/**13.8**	0.3/1.2/**1.3**	0.5/1.4/**2.3**	0.6/1.8/**3.1**	0.5/1.6/2.4

4.3 The Targeted Success rates for Transfer with Varied Targets

Following the settings in (Zhao et al., 2021), we further evaluate the performance of different calibration methods in the worse-case transfer scenario by gradually varying the target class from the highest-ranked to the lowest one.

From the results in Table 3, we can have the following findings: **1)** The three types of logit calibration methods can improve the targeted transfer success rate over the original CE. The angle-based calibration can achieve the best performance. **2)** The Temperature-based (T=5/10) and the Angle-based calibrations can outperform the Logit loss by a large margin, especially the Angle-based calibration. **3)** The margin-based calibration doesn't work well in this setting. When the target class is after 200th, the performance of margin-based will be significantly lower than the Temperature-based and Angle-based calibrations.

Table 3: Targeted transfer success rate (%) when varying the target from the high-ranked class to low.

	2nd	10th	200th	500th	800th	1000th
Logit	83.7	83.2	74.5	71.5	64.9	52.4
CE	77.4	58.6	26.9	23.7	16.7	7.0
CE/5	91.3	88.7	77.1	75.8	70.1	58.8
CE/10	89.0	87.8	81.0	79.2	73.5	62.5
Margin	87.4	81.7	61.3	51.6	43.1	23.0
Angle	92.4	89.1	80.3	79.2	76.1	66.3

4.4 THE MUTUAL BENEFITS OF DIFFERENT CALIBRATION METHODS

In this part, we evaluate the mutual benefits of combining different calibrations and can have the following findings. **1)** Combining the T=5/10/20 and Margin, there is no increase in performance compared with using one of them. This is because that the gradient directions of these two methods are very similar. **2)** Combining the T=5 and Angle, we can observe a further improvement when using ResNet50 and Dense121 as the surrogate model, *e.g.*, the transferable rate of "ResNet50 → Dense121" is increased to 82.4% with 300 iterations. Since the Angle obtains poor performance on VGG16, the transferable rates of corresponding combinations are also low in T=5/10+Angle, but T=20+Angle can deal with this issue. **3)** Combining the Margin and Angle, there are only slight improvements on ResNet50 and Dense121, while it can alleviate the negative effects caused by the angle-based calibration. Finally, by jointly considering the results in Table 1, 2 and 4, we suggest using T=5 + Angle for CNNs with more layers and the single Margin-based calibration for CNNs with fewer layers to achieve better targeted transfer attack.

Table 4: The comparison of combining logit calibrations. (The targeted transfer success rates (%) with 20/100/300 iterations are reported.)

Attack	Surrogate Model: ResNet50			Surrogate Model: Dense121		
	→Dense121	→VGG16	→Inc-v3	→Res50	→VGG16	→Inc-v3
T=5 + Margin	33.8/69.8/77.2	24.0/59.0/65.5	3.3/9.6/11.1	19.3/44.3/47.8	14.1/37.7/40.8	2.5/7.5/9.4
T=5 + Angle	34.5/74.3/**82.4**	25.6/66.5/**72.2**	3.6/10.5/**13.1**	20.3/52.7/**61.9**	15.8/45.0/**53.6**	2.3/9.2/**12.7**
T=10 + Margin	32.7/69.5/77.3	22.8/59.4/66.3	12.9/9.7/11.5	18.3/44.1/49.1	13.7/36.9/41.6	2.4/8.3/9.2
T=10 + Angle	33.0/69.8/79.1	24.4/59.0/68.9	3.4/10.0/12.9	19.4/47.2/56.1	14.8/40.1/47.0	2.5/8.3/11.0
T=20 + Margin	33.0/69.2/76.2	23.1/58.4/65.8	3.2/9.5/11.8	19.1/43.4/48.5	13.9/36.7/41.4	2.4/7.8/9.5
T=20 + Angle	34.2/68.6/76.5	24.7/58.7/66.6	3.4/9.7/12.7	20.0/44.4/50.9	15.5/38.4/43.7	2.5/8.2/9.5
Margin + Angle	34.4/70.8/78.1	24.3/60.2/67.4	3.5/10.4/12.6	19.9/46.6/52.7	15.2/39.3/44.5	2.7/8.2/9.9
Attack	**Surrogate Model: VGG16**			**Surrogate Model: Inc-v3**		
	→Res50	→Dense121	→Inc-v3	→Res50	→Dense121	→VGG16
T=5 + Margin	3.5/10.2/11.4	3.7/12.4/14.6	0.3/1.1/1.3	0.5/1.4/1.6	0.6/2.1/2.9	0.5/1.7/2.8
T=5 + Angle	2.2/2.5/2.3	2.4/2.6/2.3	0.2/0.1/0.2	0.5/1.6/**2.4**	0.6/2.0/3.1	0.5/1.7/2.5
T=10 + Margin	3.2/10.7/11.7	3.4/12.9/**15.0**	0.2/1.0/**1.4**	0.5/1.4/1.9	0.5/1.9/3.0	0.3/1.5/2.3
T=10 + Angle	3.4/6.2/5.1	3.5/7.5/7.0	0.2/0.6/0.6	0.6/1.3/1.9	0.6/2.0/3.2	0.5/1.6/2.6
T=20 + Margin	3.5/10.1/**11.8**	3.4/12.0/14.9	0.3/1.2/**1.4**	0.6/1.2/1.9	0.5/1.9/2.9	0.5/1.6/2.7
T=20 + Angle	3.2/9.7/10.1	3.9/11.9/13.3	0.3/1.0/1.2	0.6/1.6/2.0	0.6/2.0/**3.5**	0.5/1.7/**2.9**
Margin + Angle	3.3/9.8/11.1	3.5/12.6/14.6	0.3/1.2/**1.4**	0.6/1.4/2.0	0.6/1.7/3.1	0.5/1.5/2.6

4.5 TRANSFER-BASED ATTACKS ON GOOGLE CLOUD VISION

Following the evaluation protocol in Zhao et al. (2021), we randomly select 100 images to conduct a real-world adversarial attack on the Google Cloud Vision API. The attacking performance is computed based on transfer-based attacks of the ensemble of four CNNs (*i.e.*, Inc-V3, ResNet-50, Dense-121 and VGG-16). The results are shown in Table 5. We can find that the results of the Logit and CE (T=5) are very similar. But the Margin-based calibration performs worse than Logit and CE (T=5). These results reveal that our logit calibration-based targeted transfer attacks can cause a potential thread to the real-world Google Cloud Vision API.

Table 5: Non-targeted and targeted transfer success rates (%) on Google Cloud Vision API.

	Logit	CE (T=5)	Margin
Targeted	16	15	12
Non-targeted	51	53	42

5 CONCLUSION

In this study, we analyze the logit margin in different loss functions for the transferable targeted attack, and find that the margin will quickly get saturated in the CE loss and thus limits the transferablity. To deal with this issue, we introduce to use logit calibrations in the CE loss function, including Temperature-based, Margin-based, and Angle-based. Experimental results verify the effectiveness of using the logit calibration in the CE loss function for crafting transferable targeted adversarial samples. The proposed logit calibration methods are simple and easy to implement, which can achieve state-of-the-art performance in transferable targeted attack.

6 Ethics Statement

Our findings in targeted transfer attacks can potentially motivate the AI community to design more robust defenses against transferable attacks. In the long run, it may also be directly used for suitable social applications, such as protecting privacy. Contrariwise, some applications may use targeted transferable attacks in a harmful manner to damage the outcome of AI systems, especially in scenarios of speech recognition and facial verification systems. Finally, we firmly believe that our investigation in this study can provide valuable insight for future researchers by using the logit calibration for both adversarial attack and defense.

References

Jeremy Cohen, Elan Rosenfeld, and Zico Kolter. Certified adversarial robustness via randomized smoothing. In *ICML*, 2019.

Jiankang Deng, Jia Guo, Niannan Xue, and Stefanos Zafeiriou. Arcface: Additive angular margin loss for deep face recognition. In *CVPR*, 2019.

Yinpeng Dong, Fangzhou Liao, Tianyu Pang, Hang Su, Jun Zhu, Xiaolin Hu, and Jianguo Li. Boosting adversarial attacks with momentum. In *CVPR*, 2018.

Yinpeng Dong, Tianyu Pang, Hang Su, and Jun Zhu. Evading defenses to transferable adversarial examples by translation-invariant attacks. In *CVPR*, 2019.

Ian J Goodfellow, Jonathon Shlens, and Christian Szegedy. Explaining and harnessing adversarial examples. In *ICLR*, 2015.

Yiwen Guo, Qizhang Li, and Hao Chen. Backpropagating linearly improves transferability of adversarial examples. In *NeurIPS*, 2020.

Kaiming He, Xiangyu Zhang, Shaoqing Ren, and Jian Sun. Deep residual learning for image recognition. In *CVPR*, 2016.

Geoffrey Hinton, Oriol Vinyals, and Jeff Dean. Distilling the knowledge in a neural network (2015). *arXiv preprint arXiv:1503.02531*, 2015.

Gao Huang, Zhuang Liu, Laurens Van Der Maaten, and Kilian Q Weinberger. Densely connected convolutional networks. In *CVPR*, 2017.

Qian Huang, Isay Katsman, Horace He, Zeqi Gu, Serge Belongie, and Ser-Nam Lim. Enhancing adversarial example transferability with an intermediate level attack. In *CVPR*, 2019.

Nathan Inkawhich, Kevin Liang, Binghui Wang, Matthew Inkawhich, Lawrence Carin, and Yiran Chen. Perturbing across the feature hierarchy to improve standard and strict blackbox attack transferability. *NeruIPS*, 2020a.

Nathan Inkawhich, Kevin J Liang, Lawrence Carin, and Yiran Chen. Transferable perturbations of deep feature distributions. *arXiv preprint arXiv:2004.12519*, 2020b.

Alexey Kurakin, Ian Goodfellow, and Samy Bengio. Adversarial machine learning at scale. *arXiv preprint arXiv:1611.01236*, 2016.

Alexey Kurakin, Ian J Goodfellow, and Samy Bengio. Adversarial examples in the physical world. In *Artificial intelligence safety and security*, pages 99–112. Chapman and Hall/CRC, 2018.

Maosen Li, Cheng Deng, Tengjiao Li, Junchi Yan, Xinbo Gao, and Heng Huang. Towards transferable targeted attack. In *CVPR*, 2020.

Jiadong Lin, Chuanbiao Song, Kun He, Liwei Wang, and John E Hopcroft. Nesterov accelerated gradient and scale invariance for adversarial attacks. 2020.

Weiyang Liu, Yandong Wen, Zhiding Yu, Ming Li, Bhiksha Raj, and Le Song. Sphereface: Deep hypersphere embedding for face recognition. In *CVPR*, 2017.

Yanpei Liu, Xinyun Chen, Chang Liu, and Dawn Song. Delving into transferable adversarial examples and black-box attacks. In *ICLR*, 2016.

Jonathan Long, Evan Shelhamer, and Trevor Darrell. Fully convolutional networks for semantic segmentation. In *CVPR*, 2015.

Muhammad Muzammal Naseer, Salman H Khan, Muhammad Haris Khan, Fahad Shahbaz Khan, and Fatih Porikli. Cross-domain transferability of adversarial perturbations. *NeurIPS*, 2019.

Muzammal Naseer, Salman Khan, Munawar Hayat, Fahad Shahbaz Khan, and Fatih Porikli. On generating transferable targeted perturbations. In *ICCV*, 2021.

Omid Poursaeed, Isay Katsman, Bicheng Gao, and Serge Belongie. Generative adversarial perturbations. In *CVPR*, 2018.

Shaoqing Ren, Kaiming He, Ross Girshick, and Jian Sun. Faster r-cnn: Towards real-time object detection with region proposal networks. *NeurIPS*, 2015.

Karen Simonyan and Andrew Zisserman. Very deep convolutional networks for large-scale image recognition. In *ICLR*, 2015.

Christian Szegedy, Wei Liu, Yangqing Jia, Pierre Sermanet, Scott Reed, Dragomir Anguelov, Dumitru Erhan, Vincent Vanhoucke, and Andrew Rabinovich. Going deeper with convolutions. In *CVPR*, 2015.

Christian Szegedy, Vincent Vanhoucke, Sergey Ioffe, Jon Shlens, and Zbigniew Wojna. Rethinking the inception architecture for computer vision. In *CVPR*, 2016.

Florian Tramèr, Alexey Kurakin, Nicolas Papernot, Ian Goodfellow, Dan Boneh, and Patrick McDaniel. Ensemble adversarial training: Attacks and defenses. In *ICLR*, 2018.

Dongxian Wu, Yisen Wang, Shu-Tao Xia, James Bailey, and Xingjun Ma. Skip connections matter: On the transferability of adversarial examples generated with resnets. In *ICLR*, 2020.

Cihang Xie, Zhishuai Zhang, Yuyin Zhou, Song Bai, Jianyu Wang, Zhou Ren, and Alan L Yuille. Improving transferability of adversarial examples with input diversity. In *CVPR*, 2019.

Zhengyu Zhao, Zhuoran Liu, and Martha Larson. On success and simplicity: A second look at transferable targeted attacks. *NeurIPS*, 34, 2021.